Biochimica et Biophysica Acta, 1016 (1990) 177–189
Elsevier

BBABIO 43161

Light distribution, transfer and utilization in the marine red alga *Porphyra perforata* from photoacoustic energy-storage measurements *

Shmuel Malkin **, Stephen K. Herbert and David C. Fork

Carnegie Institution of Washington, Department of Plant Biology, Stanford, CA (U.S.A.)

(Received 19 June 1989)
(Revised manuscript received 24 October 1989)

Key words: Photoacoustics; Photosystem I; Photosystem II; Energy transfer; Spillover; (Marine alga)

Light energy utilization in *Porphyra perforata* was monitored by the photoacoustic method in different conditions of illumination. Auxiliary chlorophyll *a* fluorescence measurements were made to estimate the fraction of open photosystem II (PS II) reaction centers. These measurements allowed a consistent quantitation of excitation distribution and transfer from PS II to PS I under the physiological conditions used. Maximum energy storage was obtained with modulated light absorbed almost exclusively by the phycobilins (light 2). Modulated light absorbed by chlorophyll *a* (light I) gave much smaller energy storage (about 1/3 of the maximum), which could be enhanced to the maximum by addition of background light 2. Addition of increasing intensities of background light 1 to modulated light 2 did not initially induce any effect and then decreased the energy storage to about half of the maximum. From the above results and with simple mathematical modelling, numbers were obtained for light distribution and energy transfer parameters. From the enhancement saturation curves of the effect of background light 2 on the energy storage in modulated light 1 we conclude that in state 1 light 2 is exclusively absorbed in PS II and that there is no energy transfer to PS I from open PS II reaction centers. From the value of the energy storage for light 2 in state 1 and the degree of openness of PS II reaction centers it is possible to conclude that energy transfer to PS I occurs from closed PS II reaction centers with a probability approaching 1. In state 2 light 2 is distributed more evenly (approximately in a ratio PS II/PS I of 0.55:0.45) either by energy transfer via PS II from open PS II reaction centers, or by direct interactions of the phycobilins and PS I. Comparison of the maximum fluorescence values in the two states favors the second possibility. Energy transfer from PS II units with closed reaction centers occurs again in state 2 with a probability approaching 1. Comparison of energy utilization and oxygen evolution in light 1 relative to light 2 and the inhibitory effect of DCMU, which is complete in light 2 but only partial in light 1, suggests the existence of two types of PS I units: one type is engaged in electron transfer from PS II and the other type specializes in cyclic electron flow. The above quantitative analysis allows to estimate the ratio of the two types of PS I unit to be roughly about 0.3:0.7, respectively.

Introduction

In the photosynthesis of cyanobacteria and red algae, the phycobiliproteins, aggregated into the phycobilisome structure, are thought to be associated mainly with PS II and serve as its main light-harvesting pigments. Similarly, chlorophyll *a* serves mainly PS I. The quoted evidence for this is the action spectra of oxygen evolution measured with low intensity probing light in the presence of excess background light absorbed predominantly by either chlorophyll *a* or by the phycobilins. For each case the action spectrum reflects the absorption of the complementary pigments [1–3]. Another type of evidence comes from excitation spectra of fluorescence at cryogenic temperatures, particularly the comparison of the fluorescence parameters F_o and F_m at PS I and PS II emission bands [4]. Other approaches involve the rate and extent of reduction and oxidation of intersystem electron carriers [5] and action spectra for partial electron transport reactions specifically sensitized by either PS I or PS II measured in spheroplasts and isolated membranes [6].

* CIW-DPB publication No. 1040.

** On leave from the Weizmann Institute of Science.

Abbreviations: PS I, PS II, Photosystem I, Photosystem II; DCMU, 3(3,4-dichlorophenyl)-1,1-dimethylurea. See also list of symbols, p. 178.

Correspondence: S. Malkin, Biochemistry Department, The Weizmann Institute of Science, Rehovot 76100, Israel.

In contrast to the above, however, the quantum yield of steady-state oxygen evolution in cyanobacteria and red algae is found to be constant, close to the theoretical maximum, for wavelengths absorbed primarily by the phycobiliproteins (denoted light 2) [1,3,7]. This implies that light 2 excites PS I and PS II equally and that the excitation is transferred from the phycobiliproteins to PS I. The common presumption is that there is no direct interaction between the phycobiliproteins and PS I, hence it is thought that excitation from the phycobilisomes is first specifically transferred to a special chlorophyll *a* associated with PS II, and from there it is competitively transferred either to the reaction centers of PS II or to PS I [4,8]. According to this picture the yield of energy transfer to PS I should depend on the photochemical state of the reaction centers of PS II, increasing largely when the reaction centers are closed. This mechanism was proposed by Myers [8,9] and the process was termed 'spill-over'. Spill-over explains the flat quantum yield of oxygen evolution for the entire light 2 range, in spite of the differing absorption of light 2 by the phycobiliproteins and chlorophyll *a*. It is consistent with the enhancement in the quantum yield of light 2 for oxygen evolution caused by the addition of background light 1 (Emerson enhancement), by considering that when PS I receives surplus excitation (and hence causes the reaction centers of PS II to be fully opened) light 2 excitation is not transferred then to PS I but remains in PS II [9].

Another type of evidence for the above concepts emerged from the work of Butler et al. [4,10]. They observed a light induced increase of fluorescence in an emission band associated exclusively with PS I (at cryogenic temperatures) which had the same time dependence as the fluorescence rise in a PS II emission band. Since the fluorescence rise was correlated to closure of PS II reaction centers but not to closure of PS I reaction centers it was proposed that the rise of fluorescence emission from PS I reflected increased energy transfer from PS II, following the progressive closure of its reaction centers. A mathematical analysis of this phenomenon, based on data obtained at different excitation wavelengths, gave values for the energy transfer probability for open and closed PS II reaction centers as well as the initial distribution ratios of light, due to its direct absorption in PS II (β) and in PS I (α). For the alga *Porphyridium cruentum* it was first estimated [11] that the energy transfer probability was around 0.5 for an open PS II center increasing to about 1 for a closed center. The distribution ratio to PS II (β) for light absorbed almost exclusively by phycoerythrin (e.g., 580 nm) was found to be essentially 1 (i.e., total initial absorption in PS II). Similarly, the distribution ratio to PS I for light absorbed exclusively by chlorophyll *a* (e.g., 700 nm) was essentially 1 (i.e., total absorption by PS I). This work was extended [12] to take into account the two states of excitation distribution [13,14]: 'state-2' (obtained after preillumination with light 2), in which there is almost equal excitation of the two photosystems in light 2, and 'state 1' (obtained after preillumination with light 1), in which there is greater excitation of PS II than PS I in light 2. Relatively marginal differences were found in the energy transfer probabilities: 0.94 and 0.97 for states 1 and 2, respectively, for closed PS II reaction centers and 0.48 and 0.61 for open reaction centers. These numbers as such are, however, not consistent with the occurrence of significant Emerson enhancement for oxygen evolution at physiological temperatures, as is usually observed [2,3]. Probabilities of energy transfer from open PS II reaction centers to PS I close to or above 0.5 would result in an equal or less excitation in PS II relative to PS I. This would lead PS II reaction centers to be completely open and the activity of PS II could not be further enhanced by light 1. Thus, the above values of Butler and co-workers must be revised.

List of symbols

ES	energy storage (fraction of absorbed photon energy stored as chemical energy)
$(ES)_{max}$	maximum value of ES, obtained when the reaction centers of the contributing photosystem(s) are all open
E	enhancement function
E_{max}	maximum value of $E = (ES)_{max}/ES$
α, β	light distribution coefficients for light 2 in PS I and PS II, resp.
α', α''	light distribution coefficients for light 1 in PS I for linear and cyclic electron flow activities, resp.
σ', σ''	maximum energy storage contributed from PS I linear and cyclic electron flow activities, resp.
ϕ_1, ϕ_2	quantum yields of photochemistry for open reaction centers of PS I and PS II, resp.
ϕ_{ET}	energy transfer probability from a closed reaction center II to PS I
ϕ_{ETO}	energy transfer probability from an open reaction center II to PS I
f_1, f_2	degree of "openness" of PS I and PS II reaction centers, resp.
i_1	Intensity of modulated light 1
I_2	intensity of background light 2
$(I_2)_b$	intensity of background light 2, in presence of modulated light 1, at the 'balance point', where all photosystems achieve maximum activity (all reaction centers open)
F_o	fluorescence level corresponding to all PS II reaction centers open (obtained with addition of background saturating light 1)
F_s	fluorescence at a steady-state electron transport with light 2 alone (slowly varying with the state transitions)
F_m	fluorescence level corresponding to all PS II reaction centers closed (obtained with addition of photosynthetically saturating light).
k_F, k_t, k_P	decay rate constants for the excited state in PS II for fluorescence, energy transfer to PS I and photochemistry, resp.

superscripts (1) and (2) refer specifically to state 1 and 2, resp. (where no superscript appears the state designation is clear from the context)

There are indeed several weaknesses in the above analysis [11,12] of the light distribution parameters. First, it assumed that the observed initial fluorescence level (F_o), in the fluorescence induction transient, is entirely emitted from units with open reaction centers of PS II, ignoring the possibility that F_0 may contain irrelevant background contributions from other sources [15]. This could change the evaluation of energy transfer probabilities. Second, the extent of superposition of the PS I and PS II emission bands was apparently not rigorously calculated. Another obvious drawback of this approach is that cryogenic temperatures may change the structural arrangement of the pigment complexes and significantly affect the yield of energy transfer, since it is very sensitive to slight changes in distance or orientation of neighboring pigment complexes. Independent work using picosecond kinetics of the fluorescence at cryogenic temperatures, is consistent with a model which favors a much higher probability of energy transfer from chlorophyll *a* of PS II to PS I in state 2, relative to state 1. This is deduced from the decay kinetics of PS II fluorescence [16] and build-up kinetics of PS I fluorescence [17]. Quantitation of these data seems difficult, due to large noise/signal ratio. Furthermore, the extrapolation from cryogenic temperatures to the physiological conditions is again not self-evident. Thus, another type of approach is required.

In the present work, the photoacoustic method of measuring energy utilization in photosynthesis [18] was used to study excitation distribution. The photoacoustic method is applicable to physiological conditions and complementary to measurements of oxygen evolution. With the photoacoustic method one can obtain information on photosynthetic energy storage and thus quantify energy distribution. This method was used here with the marine red alga, *Porphyra perforata*. As expected, we found that light absorbed by chlorophyll *a* (light 1) results in a much lower yield of energy storage ('blue' and 'red' drop) than light absorbed by the phycobilins (light 2), and that background continuous light 2 enhances the energy storage of modulated light 1 to a maximum level. Quantitation of these results, bearing in mind the state of the system, proves that light 2 is divided between the two photosystems by a different mechanism in each state. In state 1 there is a strong dependence on the degree of closure of PS II reaction centers, implying competitive energy transfer from PS II to PS I and automatic mechanism controlled by the reaction centers to balance the photosystems (i.e., 'spill-over'). In state 2 there is excitation balance already with open PS II reaction centers either by energy transfer from open reaction centers or by direct interaction of PS I with the phycobilins. Auxiliary fluorescence measurements gave results consistent with the second possibility.

Materials and Methods

The photoacoustic method as applied to photosynthesis measurement has been outlined in numerous publications (see for example, Ref. 19 for a review). In the present study it is used to record relative changes in the conversion of light energy, absorbed by the algal thallus, to heat. The photoacoustic cell consists of a small chamber of air (of volume about 0.1 cm^3), engraved in lucite, that communicates with a microphone through a small channel. When the thallus is irradiated with intermittent light, a microphone signal is generated. This effect is primarily due to the intermittent release of heat, by the conversion of the absorbed light energy. The heat is conducted towards the thallus surface and since it is partially modulated, it generates temperature oscillations there and in the adjacent air. This in turn causes corresponding periodic pressure

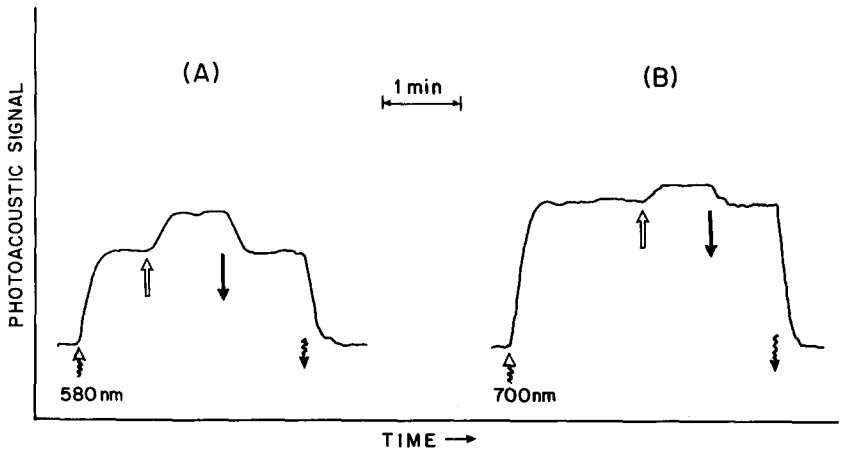

Fig. 1. Raw data of photoacoustic signals and their manipulation. Wavy arrows indicate modulated light (in the light limiting range) and straight arrows indicate background saturating white light (PAR about 2000 $\mu E \cdot m^{-2} \cdot s^{-1}$). Upward arrow – light on, downward arrow – light off. (A) Modulated light 2, 580 nm (36 $\mu E \cdot m^{-2} \cdot s^{-1}$). (B) Modulated light 1, 700 nm (90 $\mu E \cdot m^{-2} \cdot s^{-1}$). The energy storage activity, *ES*, is defined as $(a - b)/a$, where a is the signal with saturating background light and b is the signal without the background light.

oscillations (sound) in the bulk enclosed air [20]. An additional mechanism of some importance is the generation of elastic waves within the thallus itself, caused by the temperature oscillations in its bulk [21]. For a given wavelength and frequency of the intermittent light and for a given experimental material, the microphone signal is proportional to the rate of light energy absorbed and the yield of its conversion to thermal energy.

Due to photochemical activity and the partial storage of the light energy in photosynthetic intermediates, the modulated heat emitted from the alga, which produces the photoacoustic signal, is not the maximum amount. Such a maximum is obtained when the photosynthetic apparatus is saturated by additional strong non-modulated light [22,23]. Using this procedure, photochemical activity can be measured as an energy storage parameter (abbreviated *ES*). This is obtained from the difference between the photoacoustic signals in presence and absence of photosynthetically saturating background light by taking its ratio to the maximum photoacoustic signal (cf. legend to Fig. 1). The ES is theoretically the fraction of the photon energy stored as chemical energy (and therefore not released as heat) in a reaction time-scale of $1/2\pi$ of the cycle time of the intermittent light [24]. Variations in *ES* are interpreted as changes in the quantum yield of the photochemical reaction(s). To compare various wavelengths on a quantum basis, the relative yield of the reactions leading to energy storage is obtained by dividing the *ES* by the wavelength of the modulated light [22–24]. Note that the above *ES* parameter was termed 'photochemical loss' (PL) in previous publications [22–24] to indicate the deficit in the signal, relative to the maximum one, by the occurrence of photochemical reactions.

In the present case of a marine algal thallus, one would not expect the additional contribution to the photoacoustic signal by a 'photobaric' mechanism, as was found in green plant leaves [23], water ferns [25], lichens [26] or layered microalgae [27]. In those cases, the photoacoustic signal at low modulation frequencies had an additional component originating from pulsed photosynthetic oxygen evolution that also gave rise to pressure oscillations in the air phase. The thallus of *Porphyra perforata* is a single layer of cells covered with a thick (about 30 μm) cuticle saturated with water. The slow diffusion of oxygen through such a thick barrier towards the gaseous phase should result in total damping of any modulated component [23,28]. In fact, in our experiments there was no such contribution from oxygen evolution.

The set-up of the photoacoustic cell was similar to that described previously [23] with a fiber optic light delivery system. Intermittent light (frequency about 20 Hz) from a light source (ILC xenon arc R300-3)/monochromator (Bausch and Lomb)/chopper (Ithaco or PAR model 125A) combination was focused onto one of the branches of a flexible trifurcated light guide. Background light from a quartz iodine incandescent lamp (General Electric type EJM) was passed through appropriate interference filters (either Balzers type 15 nm bandwidth to achieve higher intensity, or Infra Red Industries 5 nm bandwidth to obtain greater monochromaticity). Alternatively, the light was passed unfiltered (except for a protecting heat filter, Balzers Calflex-C) to serve as a strong photosynthetically saturating background light. The background light was focused onto another branch of the light guide. The two beams were each controlled by appropriate shutters so that they could reach, separately or combined, the common light guide exit, which led light into the photoacoustic cell. The third branch of the light guide served, in a few experiments, to deliver fluorescence from the sample to a photomultiplier detector (Hamamatsu Photonics R 928). In this case fluorescence was isolated by a 685 nm narrow band interference filter, placed in front of the photomultiplier, while one or two blue Corning CS 4-96 glass filters were used to remove the red edge of the strong saturating light, so that it would not interfere with the fluorescence. The modulated signals from the microphone and the photomultiplier were processed by separate lock-in amplifiers (Ithaco model 193, PAR model 128A) which isolated the part of the signal synchronous to the light modulation frequency and thus rejected irrelevant signals and noise. The amplifier output, corresponding to the amplitude of the microphone signal, was recorded continuously on a strip chart recorder (Varian model G-1000).

The whole apparatus was placed on a heavy optical table with the photoacoustic cell particularly shielded from vibrations by putting it on heavy blocks of lead placed on a hard foam mat while the leading edge of the light guide was supported by soft foam. This was necessary as the sealed microphone is extremely sensitive to vibrations (but not to ambient sound). This arrangement was optimized by trial and error. The noise/signal ratio was still variable with time, probably dependent on factors beyond our control (e.g., activity in neighboring laboratories, earth vibrations, etc.). Thus, in most of the photoacoustic experiments a slow time constant (4 s) was used in the lock-in amplifier to bring the noise/signal ratio to reasonable low levels, appropriate for meaningful measurements.

Estimation of incident light intensities was made with a calibrated thermopile placed in the same position as the algal thallus. To estimate the ratio of absorbed light intensities for two wavelengths (particularly in the analysis of Emerson enhancement data) maximum photoacoustic signals (i.e., in the presence of photosynthetically saturating background light) were recorded for modulated beams of the two wavelengths. This maximum signal is proportional to the total absorbed light. Thus the ratio of the maximum signals is the

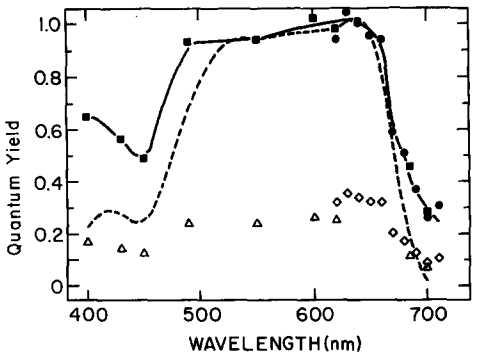

Fig. 2. The relative quantum yield of energy-storage vs. wavelength, from raw data such as in Fig. 1. The relative quantum yield is defined by the *ES*/wavelength (cf. Ref. 22). Two sets of experiments are shown (lower open points are from the original raw data), which were normalized and combined together (continuous line with the closed points). Shown for comparison is a quantum yield normalized spectrum for oxygen evolution taken from Luning and Dring [30] (dashed line).

known ratio of the incident light intensities times the ratio of the unknown percent absorption. The precision of these measurements is estimated to be within 10% error, affecting correspondingly the various calculated parameters.

Gametophytes of *P. perforata* were collected at Pescadero Point, San Mateo County, CA. 2-cm discs cut from the plants were cultured with vigorous aeration in Guillard's *f*/2 enriched sea water medium [29] changed twice weekly. Lighting was by cool-white fluorescent tubes at 25 $\mu E \cdot m^{-2} \cdot s^{-1}$ on a 12 h/12 h light-dark cycle. Temperature was 15°C. The plants were acclimated to these conditions for 7 days prior to experiments. 1-cm diameter discs of the alga were cut by a circular blade and put into the photoacoustic cell for the measurements.

Our first concern was to make sure that the algal thallus could survive and keep up photosynthetic activity while enclosed within the photoacoustic cell. The small thallus disc was moistened and adhered into a glass slide that was then clamped against the O-ring seal of the photoacoustic chamber enclosing the thallus. The same photoacoustic signals and photochemical activities persisted for hours with no obvious signs of fatigue. After the measurements were over, the disc was returned to the growth chamber and was found to keep growing normally. It seems that an equilibrium in evaporation was established rapidly in the photoacoustic cell and no further drying of the sample took place. When the alga was exposed to extensive long periods of the saturating light, the maximum level of the photoacoustic signal sometimes tended to change moderately and reversibly. This, most probably, was due to physical changes in the gross structure of the thallus, which affected the diffusion path-lengths of the released heat. However, this should not make any difference to the determination of the energy storage.

Results

Fig. 1 shows samples of raw data for the photochemical activities of the thallus, excited at two wavelengths: 580 nm, absorbed primarily by the phycobiliproteins (light 2) and 700 nm, absorbed primarily by chlorophyll *a* of PS I (light 1). The *ES* was maximum in light 2 having values usually around 0.3 with a range of 0.25–0.40 in different experiments. The *ES* for light 1 was usually about 0.1. This reflects the well-known 'red-drop' in photosynthetic activity, caused by the insufficient excitation of PS II in light 1. By making *ES* measurements over the wavelength range of 400–710 nm a relative quantum yield spectrum was constructed for photochemical activity (*ES*/wavelength), as can be seen in Fig. 2. This spectrum shows both 'red' and 'blue' drops. One can see that, in a range where the

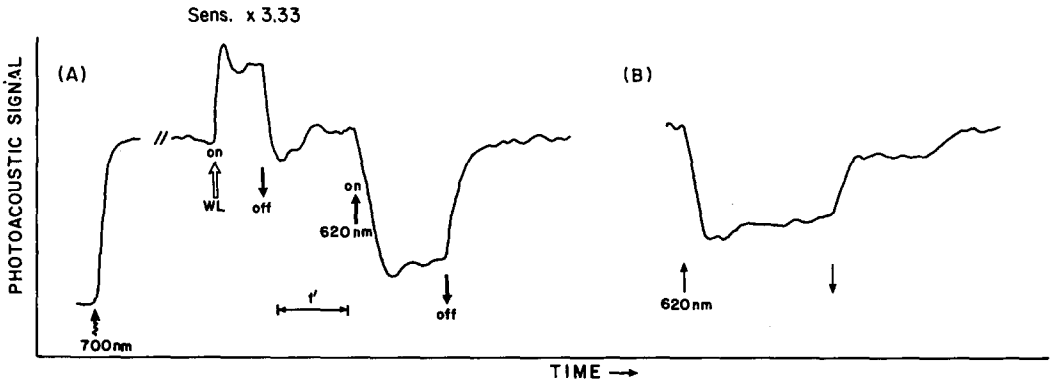

Fig. 3. Raw data for the enhancement effect of background light 2 on the *ES* measured with modulated light 1. (A) Left trace – the photoacoustic signal excited by 700 nm light (about 60 $\mu E \cdot m^{-2} \cdot s^{-1}$). Right trace – the sensitivity was increased by ×3.33 and the initial level arbitrarily adjusted by zero suppression. Notice the opposite effects induced by saturating background white light WL (increase of the signal) and by low intensity background light 2 (620 nm) (decrease of the signal). The 620 nm beam intensity was about 50 $\mu E \cdot m^{-2} \cdot s^{-1}$. The enhanced *ES* is calculated from the difference between the maximum signal and the signal in presence of light 2. (B) As in (A) but with another sample, to show the transients obtained upon switching on and off light 2.

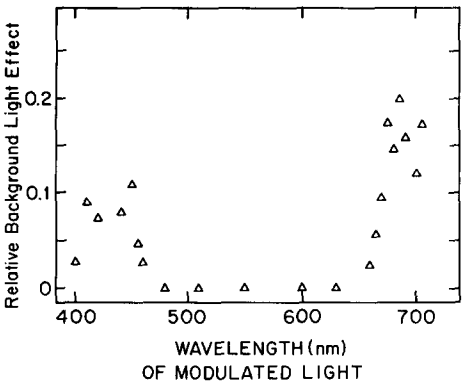

Fig. 4. The action spectrum for the enhancement of ES in varying wavelengths of the modulated light, affected by a constant background light 580 nm. The 580 nm intensity was saturating for the effect, still in the light limiting range for photosynthesis.

phycobilins have preferential absorption, the activity is maximum and quite flat. These results are consistent with reported action spectra for oxygen evolution (Refs. 2, 3, 7, 30, 31, dashed curve of Fig. 2) except that the extents of the 'red' and 'blue' drops in *ES* are significantly less than for oxygen evolution, which tends sharply close to zero in the light 1 range.

In all the above experiments we were careful to use modulated light intensities in the light limiting region for *ES* ($< 30\ \mu E \cdot m^{-2} \cdot s^{-1}$ for light 2). This was tested routinely by reducing the intensity by about 50% and observing essentially no change in *ES*. This was also confirmed by testing the range for light-limiting and light-saturating intensities, constructing a complete saturation curve for the effect of the background light (data not shown).

The *ES* activity of light 2, as recorded in Fig. 2, is presumably related to state 2, which results from adaptation to light 2. We also made a measurement for the *ES* of 580 nm immediately after 15 min adaptation to 700 nm (state 1). This resulted in an about 18% reduction of *ES* relative to state 2.

Fig. 3 shows that background light 2 caused a significant immediate decrease in the photoacoustic signal (i.e., increased energy storage) when measured with modulated 700 nm light. This demonstrates enhanced ES of modulated light 1 by background light 2. The effect tended to saturation as light 2 intensity increased, while still in the light limiting range for photosynthesis. The enhanced *ES* was calculated, as above, from the difference of the signals obtained in the presence of photosynthetically saturating background light and in

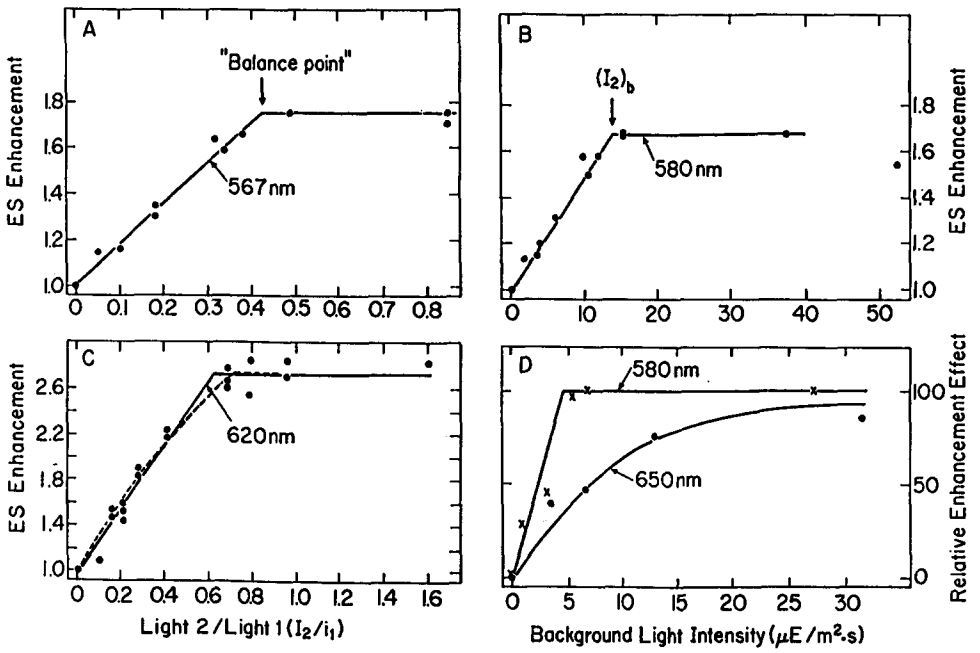

Fig. 5. Saturation curves for the *ES* enhancement effect (*ES* enhancement vs. absorbed light 2 intensity, or the ratio of absorbed intensities light 2/light 1) induced by background light 2 on the activity of modulated light 1. (A) Light 2 567 nm (max intensity $47\ \mu E \cdot m^{-2} \cdot s^{-1}$), light 1 685 nm ($28\ \mu E \cdot m^{-2} \cdot s^{-1}$). (B) Light 2 580 nm, light 1 700 nm. Light 1 intensity was not recorded but estimated roughly to be about 40–50 $\mu E \cdot m^{-2} \cdot s^{-1}$. (The absorption at 700 nm relative to that at 580 nm was about 50%). (C) Light 2 620 nm (max intensity $52\ \mu E \cdot m^{-2} \cdot s^{-1}$), light 1 700 nm ($64\ \mu E \cdot m^{-2} \cdot s^{-1}$). The solid curve is a linear plot, similar to (A) and (B). The dashed curve is a theoretical replot of the data after analysis according to a reciprocal plot and linear regression, giving a value for $\alpha/\beta = 0.176$. (D) Comparison between two light 2 saturation curves at 580 nm and 650 nm for the same sample and the same light 1 (700 nm, roughly $25\ \mu E \cdot m^{-2} \cdot s^{-1}$). 650 nm is in the border-line between light 1 and light 2 (see Fig. 2 and 5). The curve for 650 nm is drawn according to Eqn. 5a with nearly equal distribution to PS I and PS II ($\alpha/\beta = 0.82$). With this value of beta, a comparison of the initial slopes for the 650 nm and 580 nm plots supports independently the concept that 580 nm light is mainly distributed to PS II (about twice the slope as that for the 650 nm case). Expts. A–D are for different samples.

the presence of light 2 background. The saturated value of the enhanced *ES* was generally about the same as that of the *ES* obtained with modulated light 2. Fig. 3B illustrates two kinds of transient that were very often observed. One of them was a small decline in the *ES* as the irradiation with background light 2 continued (see also in Fig. 3A). The second was a small after-effect when light 2 was turned off (i.e., the *ES* did not immediately relax to the value obtained with light 1 alone; the complete transition to that value took some time). The first transient is perhaps related to a gradual decrease of the effectiveness of light 2 (due to partial transition to state 2 – indeed it disappears when the intensity of light 2 decreases). The second transient is probably related to the creation of a reduced pool of electron carriers between photosystems I and II during irradiation with light 2 allowing PS I to remain fully active with light 1 alone until the pool is oxidized.

An action spectrum of the maximum enhancement by light 2 (580 nm) of the ES in various wavelengths of modulated light, is shown in Fig. 4. In this spectrum the enhancement of *ES* by background light 2 is greatest in the red (> 660 nm) and blue (400–480 nm) regions where absorption by PS I predominates. Throughout the entire range for modulated light 2 there is no enhancement effect at all. Thus such a spectrum is an alternative means to accurately define the edges of the wavelength ranges for lights 1 and 2.

Fig. 5 shows several examples of *ES* enhancement saturation curves with light 2 at several wavelengths. The curves of Fig. 5A and B (567 and 580 nm background lights, respectively) show a linear, sharply rising light-limited region and a flat, saturated region. The linearity and the sharp transition to a plateau have a quantitative significance, as will be discussed later. Comparing different wavelengths of background light in the range of light 2 for their effectiveness in causing *ES* enhancement, it was found that the saturation value (i.e., the maximum) enhancement is always nearly the same, but the initial increasing phase differed considerably, from a linear response with maximum slope at 560–600 nm to gradually lower and lower initial slopes and deviation from linearity for longer wavelengths (compare Figs. 5A and 5B to Figs. 5C and 5D).

In remarkable contrast to the enhancement effect of background light 2 on the *ES* measured for light 1, the addition of background light 1 did not enhance the *ES* measured for modulated light 2. On the contrary, with increasing intensity of light 1 there was initially a lag (i.e., a range of intensities which did not produce any noticeable effect), while higher intensities caused a substantial decrease in the *ES*, an effect which apparently reached saturation when the *ES* decreased to about half of the original value. Fig. 6 summarizes the data in a plot of the *ES* vs. the background light 1 (685 nm) intensity. Similar results were obtained with 700 nm as

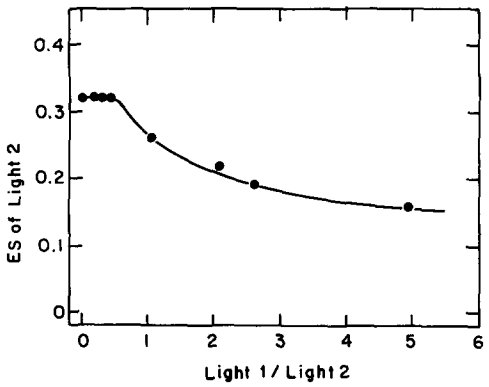

Fig. 6. Effect of background light 1 on *ES* in modulated light 2. *ES* vs. light 1 intensity.

light 1. Notice that in the experiment of Fig. 6 light intensities eventually exceed the light-limiting range, causing the slow drop in *ES* at the higher light intensities.

One must notice the contrast between the above effect and the response of oxygen evolution, measured in light 2, to light 1 addition, which results in enhancement [2,3]. The difference is significant and is due to the fact that contributions to *ES* come from both photosystems, while oxygen evolution is determined by the state of the reaction centers of PS II alone (cf. Discussion).

All the effects reported above must be related to changes in the balance of the linear electron flow between the two photosystems. Indeed when the thallus was treated with DCMU to inhibit linear electron flow, the immediate effect was a decrease of the *ES* measured in light 2 to zero (Fig. 7). However, there was still a significant degree of activity retained in light 1 (Fig. 7), but no enhancement of that activity by background light 2 (data not shown). If, following the immediate inhibiting effect, saturating white light was given, a slow process of adaptation to DCMU occurred in which

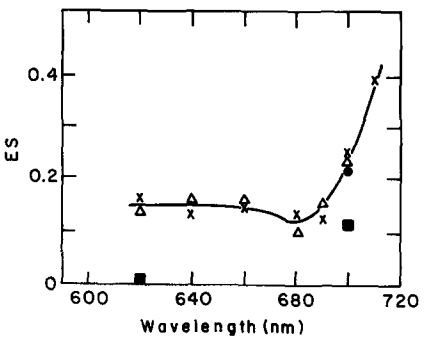

Fig. 7. The *ES* spectrum after addition of 20 μM DCMU (compare to Fig. 2). Closed squares – immediately (within 1 min) after DCMU treatment. × or △ – after an elapsion of several minutes while exposing the sample to photosynthetically saturating background light. (× – points of measurement from short to long wavelengths; △ – measurements in the reverse direction.)

photochemical activity in light 2 was partially regained (expressed by *ES* increase) (Fig. 7). Even this induced activity is probably related to PS I since its quantum yield spectrum showed a 'red rise' rather than a 'red drop' pattern; the photochemical activity in light 1, which initially was almost unaffected by DCMU, increased during the adaptation process to twice the level obtained without DCMU (Fig. 7).

In the above experiments the decision as to whether the system was in states 1 or 2 was made by considering the dominant type of irradiation given to the sample (light 2 or light 1) and its duration. To better assess the importance of the state transitions and to learn about the characteristics of states 1 and 2, we also performed room-temperature modulated fluorimetric measurements following the method outlined in Ref. 33. An example of such measurements is shown in Fig. 8. In state 2 (obtained after preillumination with light 2 alone) the parameters F_m (maximum fluorescence) and F_s (steady-state fluorescence, as is determined by the state of balance in electron flow between the two photosystems) were considerably lower than in state 1 (obtained after preillumination with light 2 and excess light 1). The parameter F_o also changed, but only slightly. The half-times of the state transitions were in the minute range, similar to the observations of Ried and Reinhardt [32]. The fluorescence parameters allowed calculation of reaction center openness in Photosystem II, i.e., the parameter f in Ref. 33, here denoted f_2 which amounted to about 0.6 in state 1 but much closer to 1 (0.8–0.9) in state 2. (An f_2 value of 1 indicates fully opened PS II centers.)

Discussion

On first sight energy storage measurements reflect phenomena previously measured by electron transport particularly the relative high efficiency in light 2, the low efficiency in light 1 and its enhancement by light 2. A closer insight, combined particularly with mathematical modelling gives, however, special significance to the energy storage data, which results in new information and also in a numerical description of how excitation is distributed. One should note that in contrast to modulated oxygen evolution rate measurements, which directly reflect both the flux of modulated excitation to PS II and the state of PS II reaction centers [34], energy storage measurements reflect contributions from all photosystems (see below). Thus the two types of measurement are complementary.

'Blue' and 'red' drops and the effect of DCMU–possible indication for two types of PS I units

The 'blue' and 'red' drops in the extent of energy storage (Figs. 1, 2) are mild relative to the reported drop in the quantum yield of oxygen evolution [3,7,31]. This difference must be accounted for by additional photochemical activity of light 1 that does not depend on PS II activity. Considering the available possibilities, energy storage in light 1 most probably reflects cyclic electron flow and the accompanying phosphorylation of ADP.

The immediate effect of DCMU (Fig. 7) is consistent with this interpretation, as DCMU only slightly inhibits energy storage in light 1, while completely inhibiting

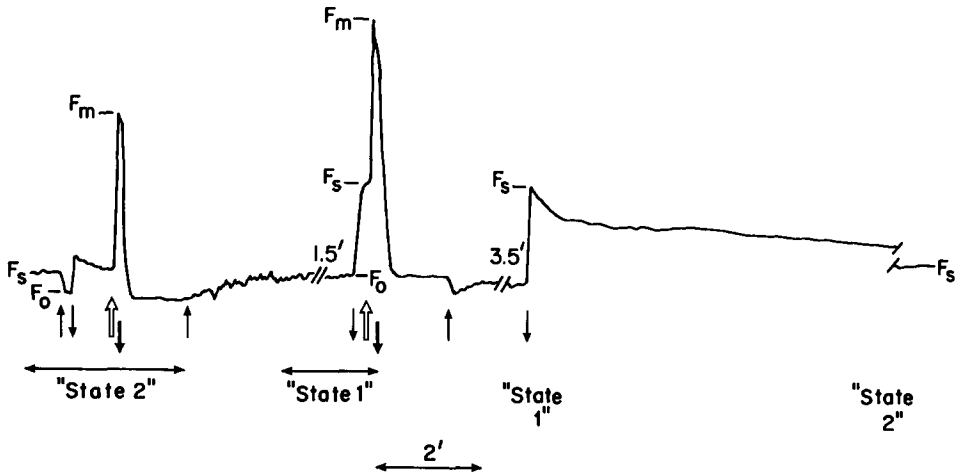

Fig. 8. Fluorescence traces obtained with modulated light 2 (580 nm) showing state 2–state 1 transitions. Thin arrows indicate the switch on (upwards) and off (downwards) of background light 1 (710 nm). Thick arrows indicate the effect of strong photosynthetically saturating broad-band light (isolated with blue 4-96 Corning filter). Fluorescence was isolated by 680 nm interference filter. Light 1 quenched the fluorescence to F_0 level while the saturating light increased the fluorescence to the F_m level. Long adaptation with light 1 brings a transition to state 1 while long adaptation to light 2 brings a transition back to state 2. These data define the fraction of open reaction centers of PS II, f_2, from $f_2 = (F_m - F_s)/(F_m - F_0)$, F_s being the steady (slow changing) fluorescence without any background light (see Ref. 33).

energy storage in light 2. Light 2 alone exhibits maximum energy storage in our studies and hence it must excite the two photosystems nearly equally for linear electron flow (see below). Since all light 2 activity is inhibited by DCMU, one concludes that light 2 itself is not engaged in any other type of photoactivity besides linear electron transport. The logical consequence is that the remaining photoactivity in light 1 in presence of DCMU results from PS I units that are not normally engaged in linear electron transport. Continuing this logic, this suggests the possibility that there is specialization among two types of PS I unit: (a) PS I units engaged in accepting electrons from PS II but not in cyclic electron flow, which receive excitation from PS II pigments and hence must be in close proximity to PS II; (b) PS I units engaged exclusively in cyclic electron flow that do not receive excitation from PS II.

With several minutes exposure to strong light, some energy storage in light 2 returns while energy storage in light 1 approximately doubles (Fig. 7). With the above assumption it turns out that this adaptive process creates structural changes in the photosynthetic membrane which allow the inhibited PS I units normally engaged in linear electron flow to store energy by gaining cyclic electron flow while retaining the ability to receive excitation from PS II by energy transfer. The conversion to cyclic flow accounts for the partial recovery of energy storage in light 2 with the doubling of energy storage in light 1 in the presence of DCMU.

Quantification of energy distribution from enhancement measurements

Evidence that light 2 is entirely distributed to PS II in state 1

Considering the above, a simple mathematical model can be formulated for the case in which modulated light 1 is the dominating irradiation and background light 2 is added briefly to measure its effect on the *ES* of light 1 (data of Fig. 5). The starting state is presumably state 1. In this state background light 2 excites the two photosystems in such a way that PS II receives a fraction β and PS I receives a fraction α of the total light 2 excitation absorbed. At low light 2 intensities, which are insufficient to achieve the maximum value of the *ES* enhancement, PS II is excited less than PS I and hence the reaction centers of PS II must be fully opened and those of PS I partially closed. This is reversed at light 2 intensities surpassing the point where saturation begins (called hereafter the 'balance' point). β (and α) will be determined from the initial phase of the saturation curve and therefore their values are relevant to a situation where PS II reaction centers are fully opened. In this initial range of light 2 intensities the balance of electron transport between the two photosystems requires:

$$(\beta - \phi_{ETO})I_2 = f_1[(\alpha + \phi_{ETO})I_2 + \alpha' i_1] \quad (1)$$

or

$$\beta I_2 = f_2(\alpha I_2 + \alpha' i_1) \quad (1a)$$

where I_2 is the absorbed intensity of light 2, i_1 the absorbed intensity of light 1 (the small letter indicates the modulated light throughout), α' is the fraction of light 1 channeled to PS I units engaged in the linear electron flow and f_1 is the fraction of open centers in that type of PS I unit. It is assumed also (in approximate agreement with the 'red' drop in oxygen evolution) that light 1 is channeled only to PS I (i.e., that PS I units engaged in the cyclic electron flow receive a fraction $1 - \alpha'$ of light 1). ϕ_{ETO} is the energy transfer probability to PS I from open PS II reaction centers. We substitute $\beta = \beta - \phi_{ETO}$ and $\alpha = \alpha + \phi_{ETO}$ for post energy transfer distribution ratios. However, since at the end of the analysis it will turn out that $\beta = 1$ for a typical light 2, hence $\phi_{ETO} = 0$ (since β cannot be larger than 1) there is no distinction between post- or pre-energy transfer distribution ratios for the case analyzed. Therefore, in the following we will use simply the letters α and β instead of α and β with this understanding. From Eqn. 1a, f_1 can be determined:

$$f_1 = \beta I_2/(\alpha I_2 + \alpha' i_1) \quad (2)$$

f_1 increases from zero as I_2 increases. f_1 is less than 1 as long as the intensity I_2 is less than an intensity $(I_2)_b$, which is the I_2 intensity at the 'balance point' (i.e., the minimum intensity that brings a balance between fully open PS II and PS I reaction centers and saturates enhancement). At the balance point, $f_1 = 1$ and $(I_2)_b$ is solved from Eqn. 2:

$$(I_2)_b = \alpha' i_1/(\beta - \alpha) \quad (3)$$

As I_2 increases further f_1 remains equal to 1, hence Eqn. 2 is rewritten to cover the whole range of I_2:

$$f_1 = \beta I_2/(\alpha I_2 + \alpha' i_1) \quad \text{for } I_2 \le (I_2)_b$$

$$f_1 = 1 \quad \text{for } I_2 \ge (I_2)_b \quad (2a)$$

For the calculation of *ES* we accept that the *ES* due to several separate photosystems is the sum of contributions from each photosystem with proper weighting factors, equal to products of the modulated light distribution fraction channeled to each photosystem (α and β), the specific energy storage for each photosystem and the fraction of open reaction centers for each photosystem. Thus, for an arbitrary photosystem if the fraction of light distribution is δ, the fraction of open

reaction centers is f and the specific maximum energy storage from this system is σ the ES contribution from that system is $\sigma\delta f$. We will denote σ' the specific energy storage in PS I units engaged in linear electron flow, σ'' the specific energy storage in PS I units engaged in cyclic electron flow and α'' the fraction of light channeled to them. At limiting light intensities the reaction centers of the units engaged in cyclic electron flow are assumed to be fully opened. Thus, the ES due to modulated light 1 is composed of the ES due to the cyclic electron flow $-\sigma''\alpha''$ – and the ES due to the linear electron flow $-\sigma'\alpha' f_1$. It follows that:

$$ES = \sigma''\alpha'' + \sigma'\alpha'\beta I_2/(\alpha I_2 + \alpha' i_1) \qquad \text{for } I_2 \le I_b$$

$$ES = ES_{max} = \sigma''\alpha'' + \sigma'\alpha' \qquad \text{for } I_2 \ge I_b \tag{4}$$

The enhancement function, E, defined as $ES/ES(I_2 = 0)$ is given correspondingly by:

$$E = 1 + (\sigma'\alpha'/\sigma''\alpha'')\beta I_2/(\alpha I_2 + \alpha' i_1) \qquad \text{for } I_2 \le I_b$$

$$E = E_{max} = 1 + \sigma'\alpha'/\sigma''\alpha'' \qquad \text{for } I_2 \ge I_b \tag{5}$$

Hence:

$$E = 1 + (E_{max} - 1)(\beta[I_2/i_1]/(\alpha[I_2/i_1] + \alpha') \qquad \text{for } I_2 \le I_b \tag{5a}$$

Eqn 5a was used to analyze the data of Fig. 5 A–D. It is evident from Eqn. 5a that, in general, a complete linearity of E vs. I_2 (or I_2/i_1) as shown in Fig. 5 A–C can be achieved only if $\alpha = 0$. In an additional analysis, considering possible error in judgment due to the scattering of the experimental points, a reciprocal plot of $(E-1)^{-1}$ vs. $(I_2/i_1)^{-1}$ for the data in Fig. 5 A–C was also made. This is expected to be linear under all circumstances. From a standard linear regression analysis of these data with proper weighting factors for individual points (points of higher E got more weighting to compensate for unproportional deviation at low $E-1$), the ratio α/β could be obtained from the intercept on the $(E-1)^{-1}$ axis and then each calculated by assuming $\alpha + \beta = 1$. This gave finally values $\alpha = 0$ (hence $\beta = 1$) for the wavelengths 567 nm (Fig. 5A) and 580 nm (Fig. 5B). For 620 nm (Fig. 5C) we found $\alpha = 0.15$ (hence $\beta = 0.85$). On the other hand, the plot for background light 650 nm (Fig. 5D) which is nearly a border wavelength between light 1 and light 2 (cf. Figs. 2 and 4) gives a curve with smooth gradual inclination towards saturation, as also expected from Eqn. 5a assuming similar values for α and β. The best theoretical curve drawn in Fig. 5D for this case corresponds to $\beta = 0.55$ and $\alpha = 0.45$. This curve also demonstrates a conclusion from Eqn. 3 that as β decreases appreciably from 1, I_b tends to a very high value (e.g., I_b tends to infinity if $\beta = \alpha$).

Calculation of the fraction of PS I units engaged in linear electron flow

The second parameter which can be obtained from the data is α'. This is achieved by the use of Eqn. 3, substituting the experimental $(I_2)_b/i_1$ and the $\beta - \alpha$ value from the previous analysis. The values found for α' at two different experiments (Fig. 5A and C) were nearly the same (0.41 and 0.46, respectively). Presumably, therefore, about 40–45% of PS I units are engaged in linear electron flow and about 55–60% in cyclic electron flow.

A more refined analysis (see next paragraph) considers that there is probably a loss of PS II quantum efficiency in state 1. One therefore should correct the above numbers for α' by multiplying them by the efficiency factor (about 0.67 – see below).

Calculation of energy transfer probabilities in state 1 and state 2

As was shown above, in state 1 and with all reaction centers of PS II open (achieved with excess light 1) light 2 (560–600) nm is exclusively absorbed and remains entirely in PS II. Thus, there is no energy transfer to PS I from open PS II centers in state 1. When light 1 is switched off about 40% of PS II reaction centers become closed (Fig. 8). Under these conditions the energy storage in light 2 is still quite high, hence one must assume that PS I receives excitation from the closed PS II reaction centers. The balanced rate equation with the above numbers is:

$$0.6\ \phi_2^{(1)} = 0.4\ \phi_{ET}^{(1)}\phi_1^{(1)} \tag{6}$$

where ϕ_1 and ϕ_2 are the quantum efficiencies for charge separation in open PS I and PS II reaction centers and ϕ_{ET} is the efficiency of energy transfer to PS I from closed PS II reaction centers. The reference to state 1 of these parameters is made by the superscript (1). Hence:

$$\phi_2^{(1)} = 0.67\,\phi_1^{(1)}\,\phi_{ET}^{(1)} \tag{6a}$$

Assuming that the specific contribution of each photosystem to the ES parameter is roughly equal (as also indicated in Fig. 6), one obtains, accounting for light distribution and efficiency:

$$ES = ES_{max}(0.6\ \phi_2^{(1)} + 0.4\ \phi_{ET}^{(1)}\phi_1^{(1)}) = ES_{max}\ 0.8\ \phi_{ET}^{(1)}\ \phi_1^{(1)} \tag{7}$$

(cf. Eqn. 6).

We find (see Results) that under these conditions (light 2 in state 1) ES is indeed about 0.8 of the maximum (light 2 in state 2). It follows therefore that $\phi_1^{(1)}$ and $\phi_{ET}^{(1)}$ must both be equal to about 1 and hence $\phi_2^{(1)}$ is equal to 0.67. (This lower efficiency explains why PS II reaction centers are closed only to the extent of 0.4 rather than

the full extent of 0.5 required for a true 'spill-over' mechanism.)

Similar arguments will be applied for state 2. In this state about 0.9 of PS II centers are open (Fig. 8). Since electron transport is nearly optimal one must consider either energy transfer to PS I from open PS II reaction centers (with efficiency ϕ_{ETO}) or alternatively direct light excitation of PS I by the phycobilins. Considering the first case, the balanced rate equation takes the following form:

$$0.9\,(1-\phi^{(2)}_{ETO})\,\phi^{(2)}_2 = (0.1\,\phi^{(2)}_{ET} + 0.9\,\phi^{(2)}_{ETO})\,\phi^{(2)}_1 \qquad (8)$$

where the reference to state 2 is made by the superscript (2). The equation for ES is therefore:

$$ES = ES_{max}\,1.8\,(1-\phi^{(2)}_{ETO})\,\phi^{(2)}_2 \qquad (9)$$

Considering Fig. 6, which shows no change of ES in light 2 by addition of light 1 at the low intensity range, we may assume that since at the point of balance, where all reaction centers of both photosystems are open and energy utilization is maximum it is also maximum with light 2 alone. State 2 is considered to be most efficient also in terms of electron transport. Thus for this state we assume $\phi^{(2)}_1 = \phi^{(2)}_2 = 1$ and $ES = ES_{max}$. We therefore obtain simplified version of Eqns. 8 and 9 with only $\phi^{(2)}_{ETO}$ and $\phi^{(2)}_{ET}$ as unknowns. The solutions for these unknowns follow directly: $\phi^{(2)}_{ETO} = 0.445$ and $\phi^{(2)}_{ET} = 0.999$.

Assuming the second case for state 2, namely a passive distribution of light by direct absorption in the phycobilins (with initial distribution ratios β and α to PS II and PS I, respectively) and no energy transfer from open centers of PS II, the balanced rate equation is:

$$0.9\,\beta^{(2)} = \alpha^{(2)} + 0.1\,\phi_{ET}\,\beta^{(2)} \qquad (10)$$

The equation for ES is therefore:

$$ES = ES_{max}\,(1.8\cdot\beta^{(2)}) \qquad (11)$$

Eqns. 10 and 11 are completely equivalent to Eqns. 8 and 9 by replacing $\beta^{(2)}$ with $1-\phi^{(2)}_{ETO}$ and $\alpha^{(2)}$ with $\phi^{(2)}_{ETO}$. Since $\alpha^{(2)} + \beta^{(2)} = 1$ these two equations yield again the same solutions: $\beta^{(2)} = 0.555$; $\alpha^{(2)} = 0.445$ and $\phi^{(2)}_{ET(2)} = 1$. The results of all the above calculations, including the two possibilities in state 2, are summarized in Table I.

It appears that in both possibilities and for open PS II reaction centers a fraction (0.445) of light 2 is active in PS I. It is thus impossible from the photoacoustic data alone to discriminate between energy transfer via PS II or direct absorption by the phycobilins by PS I. Consideration of fluorescence data for F_m, however, argues more in favor of the second possibility of passive, roughly equal, light 2 distribution in state 2, as the first possibility leads to a major inconsistency, as follows: considering the first possibility only, since with closed PS II centers energy transfer is the dominant process ($\phi_{ET} \approx 1$) one may approximately write $F_m = k_F/k_t$ for both states 1 and 2, where k_F and k_t are the excited state decay rate constants for fluorescence and energy transfer, respectively. Fig. 8 shows that the ratio F_m (state 2)/F_m (state 1) is about 0.7, indicating that k_t in state 1 is 0.7 that of k_t in state 2, bearing in mind that k_F is invariant. However, this small reduction in k_t is not enough to explain the drastic change of the energy transfer yield, ϕ_{ETO}, from about 0.445 (state 2) to zero (state 1). The energy transfer yield probability for open reaction centers is approximately $k_t/(k_t + k_p)$, where k_p is the rate constant for photochemistry. From the above, k_t in state 2 is estimated to be about 0.8 of k_p and hence k_t in state 1 is about 0.56 of k_p, leading to an energy transfer yield for open reaction centers in state 1 of about 0.36, clearly in gross contradiction to our data indicating zero energy transfer.

Considering the lower efficiency of $\phi^{(2)}_2$ in state 1 the previous analysis on the light distribution in state 1 should be modified by replacing β with $\phi^{(1)}_2\beta$, starting from Eqn. 1. In this case the quoted numbers for the ratio α/β should be applied to $\alpha/\phi^{(1)}_2\beta$. The conclusion that $\alpha = 0$ in light 2 does not change, evidently. A more serious correction should be applied to the estimation of

TABLE I

Light distribution to PS II (β) and probabilities of energy transfer to PS I (ϕ_{ET} and ϕ_{ETO})

	State 1			State 2			
	β	ϕ_{ETO}	ϕ_{ET}	β		ϕ_{ETO}	ϕ_{ET}
Porphyridium cruentum Ley and Butler [12]	1	0.48	≈1	1		0.61	≈1
Porphyra perforata This work	1	0	(a) ≈1 (b)	0.55 1	0 0.45	≈1 ≈1	

[a] More favored possibility.
[b] Less favored possibility (see text).

α', since this depends on $\beta - \alpha$ (Eqn. 3) which should be replaced by $\phi_2^{(1)}\beta - \alpha$. In the analyzed case, $\alpha = 0$, hence the former values for α' should be multiplied by $\phi_2^{(1)}$ (≈ 0.67).

The effect of background light 1 on the ES in modulated light 2

The above estimations are approximately consistent with the drop in the *ES* of light 2 (in state 2) by background light 1 in the higher intensities range above a threshold (Fig. 6). This presumably reflects partial inhibition of energy storage of light 2 by closure of PS I reaction centers. Hence this phenomenon indicates independently that a considerable fraction of light 2 (roughly half) is channeled irreversibly to PS I, while presumably PS II reaction centers are fully opened. The contribution to the total *ES* from this fraction of light 2 diminishes gradually to zero as PS I becomes progressively closed. It should be noted that in the higher intensity range of this experiment there is probably some further contribution to the decrease of ES due to partial approach to photosynthetic saturation.

In contrast to this phenomenon, which is peculiar to energy storage measurements, is the positive Emerson enhancement in oxygen evolution exerted by non modulated light 1 on modulated light 2, as is usually observed. This is because the observed modulated rate depends on the degree of openess of PS II reaction centers which increase upon light 1 addition. As noted above, *ES* depends on the state of reaction centers of both PS I and PS II.

Summing up

The above analysis represents most direct evidence, applicable to physiological conditions, that in state 1 and when PS II reaction centers are fully opened (in the presence of excess background light 1) light 2 absorbed by the phycobiliproteins is directed exclusively into PS II and is not transferred to PS I. However, light 2 still shows appreciable energy storage activity in state 1 (82% relative to state 2) immediately when light 1 is switched off, which points to an immediate redistribution of excitation by energy transfer. Indeed, under these conditions PS II reaction centers become closed due to the initial imbalance of excitation and energy transfer can occur from closed PS II reaction centers. The extent of closure is controlled by the final achievement of balanced excitation of the two photosystems. This is a true 'spill-over' mechanism in the original sense (9). One can calculate that ideally an even distribution by the 'spill-over' mechanism is reached when the reaction centers of PS II are closed to an extent of 50%, provided that the energy transfer efficiency from a closed reaction center is 1. This is indeed consistently close to the fluorescence data for state 1 (Fig. 8) showing an extent of PS II reaction centers closure of about 38%. In state 2, light 2 is essentially distributed equally to the two photosystems (maximum energy storage) for open PS II reaction centers. The fluorescence data (Fig. 8) indeed show that the reaction centers of PS II are mostly open, indicating no drive for their closure that would be otherwise created in a state of imbalance. This is also seen from the effect of light 1 to decrease the energy storage of light 2 to about half (Fig. 6).

Possible relevance to other work

It appears, therefore, that in both states with light 2 alone there are energy transfer interactions leading ultimately to equal excitonic distribution. However, this is achieved in two different ways: in state 1 by energy transfer from closed PS II reaction centers only and in state 2 by either direct excitation of PS I from the phycobilisomes (the more favorable assumption) or as a result of increased PS II–PS I interaction enabling energy transfer to PS I to compete almost equally with energy transfer to an open PS II reaction center (the less favorable assumption). The interaction between the photosystems in state 1 is such that energy transfer to PS I cannot compete well with energy trapping at an open PS II reaction center but competes successfully in closed reaction centers with both radiative and radiationless transitions. These conclusions are at variance with Ley and Butler [12], as mentioned in the Introduction. A comparison between their and our conclusions is given in Table I.

It is interesting to note the smaller energy-storage, of light 2 alone, in state 1 relative to state 2 (by about 18%). In our analysis this is traced to a significant inherent loss of PS II efficiency for electron transport in open reaction centers. This conclusion is consistent with a smaller extent (0.38) of reaction center closure in state 1 than expected in an ideal case (0.5). One should not confuse, however, the above inefficiency with the overall smaller efficiency for oxygen evolution of higher plants in state 1 relative to state 2 [35]. The smaller efficiency there is traced to the imbalance of the photosystems and the resulting closure of PS II reaction centers, which is not compensated, as here, by energy transfer to PS I. More relevant perhaps is the work of Williams and Salamon [36] on oxygen evolution enhancement measurements in *Chlorella* which were generally interpreted by changes in inherent quantum yields of the photosystems. Reexamination of their B-type signals may lead to a similar interpretation as here and explained by a simultaneous increase in β in the transition to state 1 compensated by a loss of quantum efficiency in PS II.

Previous observations on *Porphyra perforata* [37] can partly be integrated in terms of the present model. The PS I emission changes seen at cryogenic temperatures

[37] could be rationalized by small differences in PS II–PS I energy transfer probabilities from closed reaction centers in states 1 and 2. The increased activity of light 2 in state 2 for cytochrome oxidation in presence of DCMU is also due to somewhat increased probability of energy transfer from a closed reaction center. The increased activity in state 1 for fluorescence induction results from a combination of about 2-fold higher excitation rate in PS II compensated partly by the previously mentioned decrease of PS II efficiency. The changes in PS II emission are too extensive to explain by changes in energy transfer. They could be partly due to changes in structure leading to changes in the radiationless decay constant. *

A further conclusion from this work is that of PS I specialization – different PS I units have different functions (cyclic phosphorylation; linear electron flow). This conclusion may be general for phycobilisomes containing algae. It is interesting to note a consistency with the low stoichiometric ratios of PS II/PS I between 0.2 and 0.7 (depending on ambient illumination) found in cyanobacteria [38,39]. It is quite tempting to interpret our value of the fraction of PS I units involved in linear electron flow (i.e., α') in terms of the above stoichiometric ratio, by assuming that each PS I unit associated with linear electron flow is attached to a PS II unit in a 1 : 1 ratio. According to the original previous analysis the average α' is about 0.43. Taking into account the reduction in PS II activity (i.e., $\phi_2\beta \approx 0.67$ for light 2, $\alpha = 0$) the use of Eqn. 3 would give $\alpha' \approx 0.29$. This number is within the common range found for PS II/PS I stoichiometry [38,39].

References

1 Jones, L.W. and Myers, J. (1964) Plant Physiol. 39, 938–946.
2 Ried, A., Hassenberg, B., Metzler, H. and Ziegler, R. (1977) Biochim. Biophys. Acta 459, 175–186.
3 Fork, D.C. (1963) in Photosynthetic Mechanisms of Green Plants (Kok B. and Jagendorf A., eds.), pp. 353–361, NSF-NRC Publ. 1145 Washington, DC.
4 Ley, A.C. and Butler, W.L. (1977) in Photosynthetic Organelles. Plant Cell Physiol. special issue, No. 3 (Miyachi, S., Katoh, S., Fujita, Y. and Shibata, K., eds.), 33–46.
5 Duysens, L.N.M. and Amesz, J. (1962) Biochim. Biophys. Acta 64, 243–260.
6 Tel-Or, E. and Malkin, S. (1977) Biochim. Biophys. Acta 459, 157–174.
7 Luning, K. and Dring, M.J. (1985) Marine Biol. 87, 119–129.
8 Myers, J. and Graham, J-R. (1963) Plant Physiol. 38, 105–116.
9 Myers, J. (1963) in Photosynthetic Mechanisms of Green Plants (Kok, B. and Jagendorf, A., eds.), pp. 301–317. NSF-NRC Publ. 1145 Washington DC.
10 Butler, W.L. (1978) Annu. Rev. Plant Physiol. 29, 345–378.
11 Ley, A.C. and Butler, W.L. (1977) Proc. Natl. Acad. Sci. (USA) 73, 3957–3960.
12 Ley, A.C. and Butler, W.L. (1980) Biochim. Biophys. Acta 592, 349–363.
13 Fork, D.C. and Satoh, K. (1986) Annu. Rev. Plant Physiol. 37, 335–361.
14 Biggins, J., Bruce, D. and Gibbs, P.B. (1989) in Toward a broad understanding of photosynthesis – multiple approaches to a common goal (Briggs, W., ed.), pp. 363–374, Alan R. Liss, New York.
15 Malkin, S. and Siderer, Y. (1974) Biochim. Biophys. Acta 368, 422–431.
16 Bruce, D., Biggins, J., Steiner, T. and Thewalt, M. (1985) Biochim. Biophys. Acta 806, 237–246 (1985).
17 Bruce, D., Hanzlik, C.A., Hanock, L.E., Biggins, J. and Knox, R.S. (1986) Photosyn. Res. 10, 283–290.
18 Cahen, D., Bults, G., Garty, H. and Malkin, S. (1980) J. Biochem. Biophys. Methods 3, 293–310.
19 Buschmann, C., Prehn, H. and Lichtenthaler, H. (1984) Photosyn. Res. 5, 29–46.
20 Rosencwaig, A. and Gersho, A. (1976) J. Appl. Phys. 47, 64–69.
21 McDonald, F.A. and Wetsel, G.C., Jr. (1978) J. Appl. Phys. 49, 2312–2322.
22 Lasser-Ross, N., Malkin, S. and Cahen, D. (1980) Biochim. Biophys. Acta 593, 330–341.
23 Bults, G., Horwitz, B.A., Malkin, S. and Cahen, D. (1982) Biochim. Biophys. Acta 679, 452–465.
24 Malkin, S. and Cahen, D. (1978) Photochem. Photobiol. 29, 803–813.
25 Kulasooriya, S.A., Arad, H., Canaani, O., Tel-Or, E. and Malkin, S. (1988) Symbiosis 6, 117–128.
26 Canaani, O., Ronen, R., Garty, J., Cahen, D., Malkin, S. and Galun, M. (1984) Photosyn. Res., 5, 297–306.
27 Canaani, O. (1986) Biochim. Biophys. Acta 852, 74–80.
28 Poulet, P., Cahen, D. and Malkin, S. (1983) Biochim. Biophys. Acta 274, 433–446.
29 Mclachlan, J. (1973) in Handbook of Phycological Methods (Stein, J.R., ed.), pp. 25–52, Cambridge University Press, London.
30 Govindjee (1963) in Photosynthetic Mechanisms of Green Plants (Kok, B. and Jagendorf, A., eds.), pp. 318–334, NSF-NRC Publ. 1145, Washington, DC.
31 Haxo, F.T. and Blinks, L.R. (1950) J. Gen. Physiol. 33, 389–422.
32 Ried, A. and Reinhardt, B. (1977) Biochim. Biophys. Acta 460, 25–35.
33 Malkin, S., Telfer, A. and Barber, J. (1986) Biochim. Biophys. Acta 848, 48–57.
34 Joliot, P. (1967) in: Energy Conversion in the Photosynthetic Apparatus. Brookhaven Symp. in Biology No. 19. pp. 418–433, Brookhaven Natl. Lab/Associated Universities.
35 Canaani, O. and Malkin, S. (1984) Biochim. Biophys. Acta 766, 513–524.
36 Williams, W.P. and Salamon, Z. (1976) Biochim. Biophys. Acta 430, 282–299.
37 Satoh, K. and Fork, D.C. (1983) Biochim. Biophys. Acta 722, 190–196.
38 Manodori, A. and Melis, A. (1987) in Progress in Photosynthesis Research (Biggins, J., ed.), Vol. II, pp. 249–252, Martinus Nijhoff, Dordrecht.
39 Manodori, A. and Melis, A. (1986) Plant Physiol. 82, 185–189.

* In Ref. 37 the dark state is called state 2 and the state achieved after adaptation to light 2 is called state 3. In the present paper we do not refer to the dark state in particular and prefer to use the more 'classical' definition of state 2.